

Structural and Optical Studies of Potential Ferroelectric Crystal: KDP Doped TGS

P. R. Deepti^{1*} and J. Shanti²

¹Department of Physics, The Oxford College of Engineering, Bangalore, Karnataka, India-560068

²Department of Physics, Avinashilingam University for Women, Coimbatore, Tamilnadu, India-641038

Received 13 October 2013, accepted in final revised form 19 December 2013

Abstract

Triglycine sulphate (TGS), an important ferroelectric material has been widely used in the fabrication of high sensitivity infrared detectors at room temperature. Single crystals of KDP doped TGS was grown by slow evaporation method at room temperature in this study. The grown crystal was characterized by UV-Vis spectroscopy, FTIR spectroscopy, powder X-ray diffraction studies, and ferroelectric studies. KDP doped TGS crystals were found to be highly transparent and full faced. The experimental results evidence the suitability of the grown crystal for optoelectronic applications.

Keywords: Crystal growth; KDP-doped TGS; Ferroelectric studies

© 2014 JSR Publications. ISSN: 2070-0237 (Print); 2070-0245 (Online). All rights reserved.

doi: <http://dx.doi.org/10.3329/jsr.v6i1.16584> J. Sci. Res. **6** (1), 1-9 (2014)

1. Introduction

Triglycine sulphate plays a major role in FT-IR instrumentation and infrared detector. It exhibits order disorder phase transition at the Curie point 49°C. TGS has protonated carboxyl groups and form chain-like system with SO_4^{2-} group. The neighbouring chains are connected by SO_4^{2-} groups of adjacent chains and GI group. Such configuration of TGS is regarded as particularly important for the ferroelectric behavior of TGS crystal. The spontaneous polarization reversal in TGS is due to the proton transfer between glycine and glycinium ions [1-2]. TGS exhibits order-disorder phase transition at the Curie point. Above Curie temperature, it is in the Paraelectric phase with space group symmetry $P2_1/m$ and below Curie it is in the ferroelectric phase with space group symmetry $P2_1$ with two formula units per unit cell [3]. All ferroelectric materials are pyro electric, however, not all pyro electric materials are ferroelectric. Below Curie temperature, ferroelectric and pyro electric materials are polar and possess a spontaneous

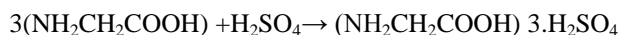
*Corresponding author: shanthinelson@gmail.com

2 Structural and Optical Studies

polarization or electric dipole moment [4-7]. However, this polarity can be reoriented or reversed fully or partially through the application of an electric field with ferroelectric materials. TGS has a major disadvantage that it is depolarized by thermal, mechanical, and electrical means. In order to overcome this difficulty, several studies have been attempted with different organic and inorganic dopants to achieve effective internal bias to stabilize the domains to increase the pyro electric and ferroelectric properties of TGS crystals [8–14]. In this article, we report the effect of doping TGS crystal with potassium di hydrogen phosphate (KDP), and the characterization studies adopted for the grown crystal.

2. Materials and Methods

Analar grade reagent (AR) L- Glycine and concentrated sulphuric acid (H_2SO_4) of 99% purity were dissolved in deionized water in the molar ratio of 3:1, and the solution was heated upto $50^{\circ}C$ to obtain TGS salt. Glycine reacts with sulphuric acid as follows:



The synthesized salt was again dissolved in double distilled water and then recrystallized by natural evaporation process. This process was repeated twice to improve the purity of the material. To obtain doped TGS crystal, 1mole% KDP was added to the saturated mother solution. Highly transparent and full faced crystals were obtained within two weeks. The KDP doped TGS crystals are found as colorless and are shown in Fig 1.

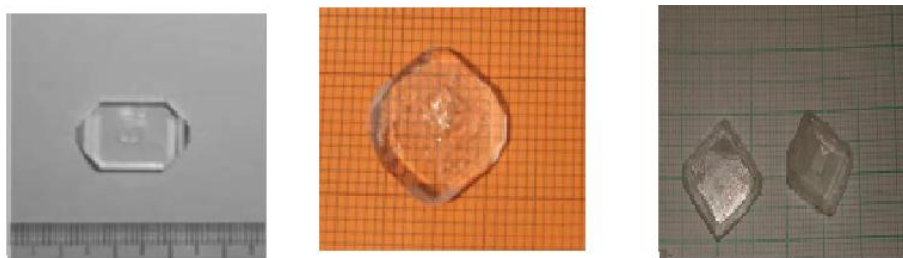


Fig. 1. Photograph of (a) pure KDP , (b) pure TGS, and (c) KDP doped TGS crystal.

TGS may be called glycine-di glyciniumsulphate with chemical formula $(NH_3^+CH_2COO^-)(NH_3^+CH_2COOH)_2 SO_4^{2-}$. Of the three glycine groups contained in the asymmetric unit, two assume a completely planar configuration and the third one assumes a partially planar configuration. The bond between two planar groups II and III are responsible for ferroelectric transition. Above the Curie temperature, glycine I molecule is split. Reversal of the polarization in the material is largely associated with the rotation of the glycine I group about the crystallographic ‘a’ axis to change into its mirror image [15].

3. Results and Discussion

3.1. UV-Vis spectral analysis

The optical transmission spectra of the grown crystal were carried out in the range of 200nm 800nm covering the entire near-ultraviolet, visible, and near infrared region using SHIMADZU UV-160 Spectrometer to find the transmission range about the suitability of this grown crystal for optical applications. An optically polished single crystal was used for this study. The transmission spectra for pure KDP and KDP doped TGS are shown in Fig. 2. A strong absorption and the UV cut off wavelength lies at 270 nm for KDP-doped TGS crystal, and it reveals the good optical quality of the grown crystal. High transmission in the entire visible region for KDP-doped TGS crystal proves the suitability of grown crystal as UV tunable laser and in second harmonic generation (SHG) device applications. The band gap calculated using the formula, $E_g = hc/\lambda$ is found to be 4.6 eV. The absence of absorption and excellent transmission in entire visible region makes this crystal a good candidate for optoelectronic application [16–18].

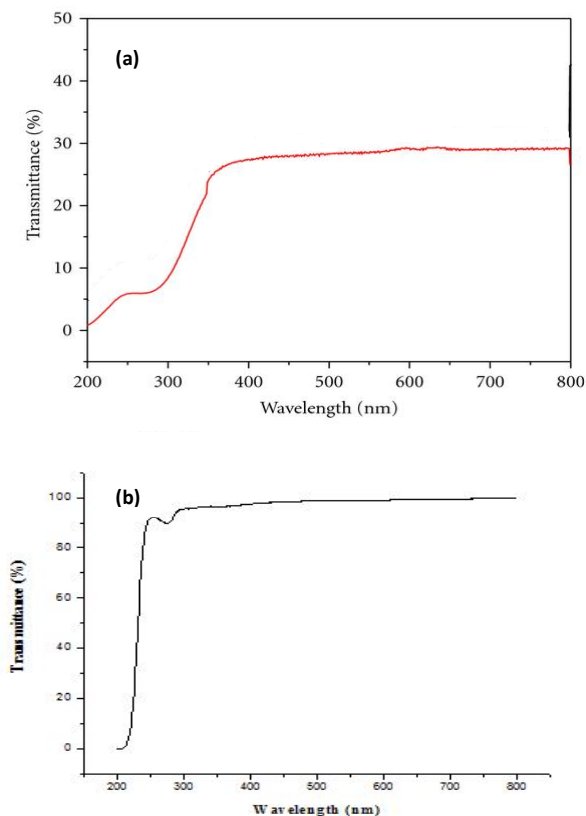


Fig. 2. Transmission spectra of (a) pure KDP and (b) KDP doped TGS crystal.

3.2. Powder x-ray diffraction

X-ray diffraction technique is a powerful tool to analyze the crystalline nature of the materials. If the material to be investigated is crystalline, well defined peaks will be observed. Powder X-ray diffraction analysis was carried out by using PANalytical X-Ray diffractometer with a $\text{CuK}\alpha$ radiation. The sample was scanned over the range 20° - 70° . The XRD pattern of pure KDP and KDP doped TGS crystal is shown in Fig. 3(a) and 3(b). The structural data for pure KDP and KDP doped TGS are given in Table 1.

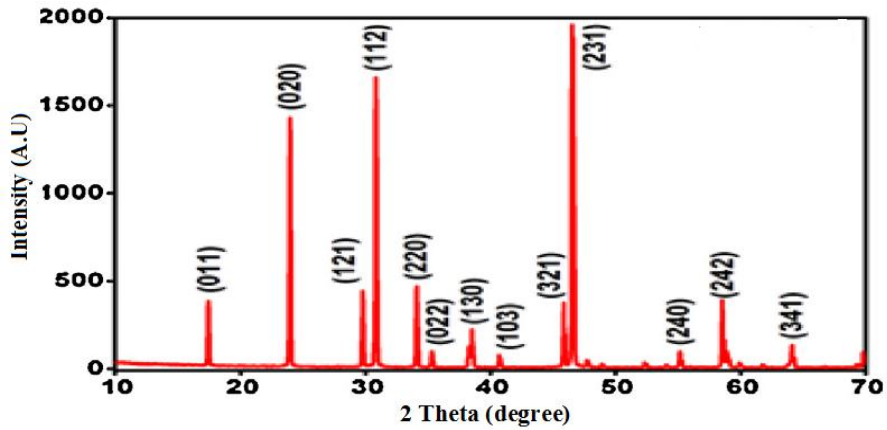


Fig. 3(a). Powder XRD pattern of pure KDP crystal.

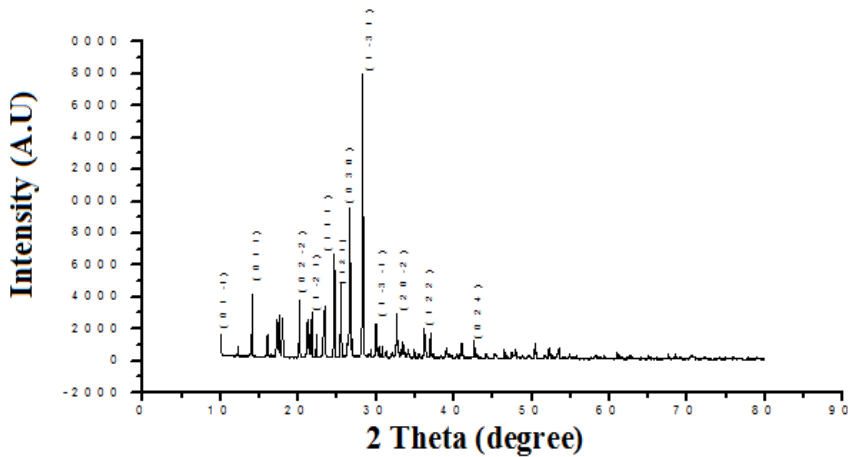


Fig. 3(b). Powder XRD pattern of KDP doped TGS crystal.

Table 1. The structural data for pure KDP and KDP doped TGS.

Lattice parameters	Pure KDP	KDP doped TGS
a	7.436 Å	5.732 Å
b	7.436 Å	12.622 Å
c	6.979 Å	9.163 Å
α	90°	90°
β	90°	105.47°
γ	90°	90°
V	385.92 Å ³	638.92 Å ³
Structure	Tetragonal	Monoclinic

3.3. FTIR spectral study

The infrared spectral analysis is effectively used to understand the chemical bonding and it provides information about molecular structure of the synthesized compound. Fourier transform infrared spectra were recorded in the range 400-4000cm⁻¹ using Perkin Elmer spectrophotometer. The sample used was in pellet form mixed with KBr. The characteristic absorption peaks are observed in the range from 400-4000cm⁻¹ IR and is shown in Fig. 4.

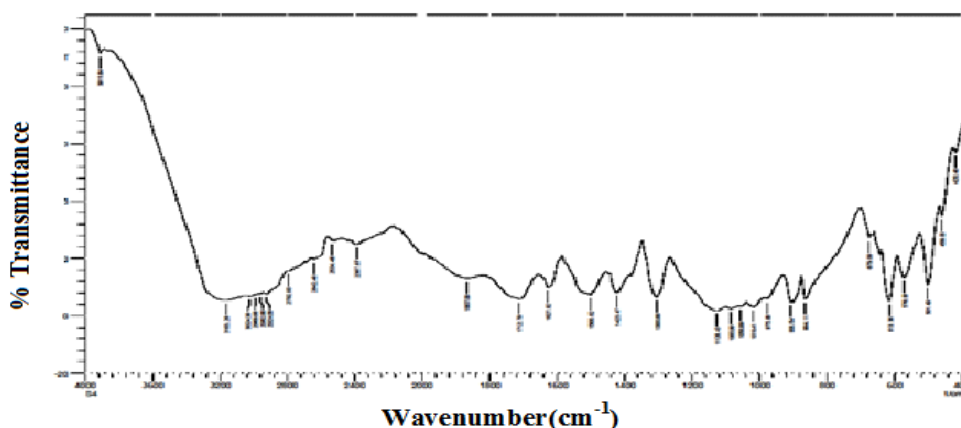


Fig. 4. FTIR spectra of KDP doped TGS crystal.

The NH, OH and CH absorption occurs at around high frequency of 3163cm^{-1} . The spectra at 1627cm^{-1} is assigned for NH_2 bending. The absorption in the range $1712\text{-}1867\text{cm}^{-1}$ is assigned to C=O stretching of carboxylic acid. The broad band around 1100cm^{-1} is assigned to C-N asymmetric stretch of SO_4 . The peak absorption at 613cm^{-1} and 501cm^{-1} are due to NH_3 oscillation. The observed frequencies and their assignments for KDP doped TGS crystal are compared with those of pure KDP and listed in Table 2.

Table 2. Frequencies and their assignments for pure TGS and KDP doped TGS crystal.

Pure TGS	KDP doped TGS	Assignments
3173	3163	(NH_3^+) symmetric stretching
2914	2924	CH_2 stretching
2619	2642	CH_2 stretching
1714	1712	Overtone and combinations
1611	1620	Amide
1518	1500	(NH_3^+) anti symmetric bending
1416	1423	NH_i bending+ NH_3 symmetric bending
1323	1303	CO_2 symmetric stretching+ CH_2 twisting
1121	1126	NC_2^α stretching + NC_3^α stretching
901	906	C-C stretching
616	613	C_2 out of plane bending + C_2N torsion+ C_1O out of plane bending
505	501	NH_3 oscillation

3.4. Photoconductivity studies

Photoconductivity measurements were made using Keithley 485 picoammeter. The dark current was recorded by keeping the sample unexposed to any radiation. Fig. 5 shows the variation of both dark current (I_d) and photocurrent (I_p) with applied field. It is seen from the plots that both I_d and I_p of the sample increase linearly with applied field. It is observed from the plot that the dark current is always higher than the photo current, thus confirming the negative photoconductivity. The phenomenon of negative photoconductivity is explained by Stockmann model [19]. The negative photoconductivity in a solid is due to the decrease in the number of charge carriers or their lifetime, in the presence of radiation [20]. For a negative photoconductor, forbidden gap holds two energy levels in which one is placed between the Fermi level and the conduction band while the other is located close to the valence band. The second state has higher capture cross-section for electrons and holes. As it captures electrons from the conduction band and

holes from the valence band, the number of charge carriers in the conduction band gets reduced and the current decreases in the presence of radiation.

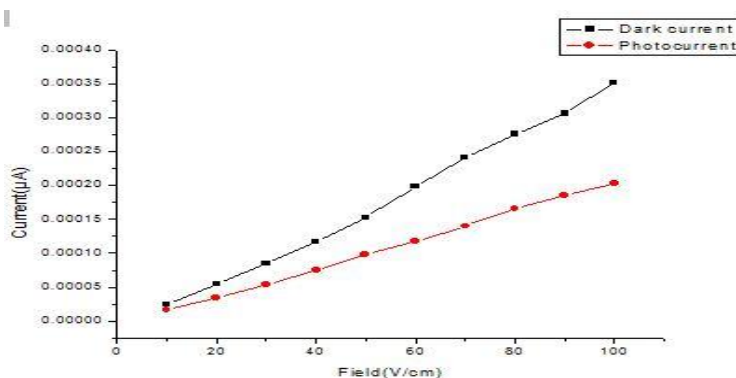


Fig. 5. Variation of dark current (I_d) and photocurrent (I_p) with applied field.

3.5. Ferroelectric P - E hysteresis loop analysis

The properties of ferroelectrics are governed by their crystallographic structure [21- 23] and strongly influenced by the lattice defects, presence of which in crystals leads to appearing and existence of internal bias field [24]. The polarization and electric field (P - E) curve was traced in KDP doped TGS crystals using a standard computer controlled Sawyer-Tower P - E hysteresis analyzer. A good quality crystal was used for the study. The opposite faces were electroded with conducting silver paste. Typical ferroelectric P - E hysteresis loop of grown KDP doped TGS crystal is shown in Fig. 6. It is found that the crystals were able to sustain a field (E_c) up to 5 kV/cm. In addition, a well saturated hysteresis loop was obtained in the grown KDP doped TGS crystal. Higher field was not applied to avoid the damage of the TGS crystal.

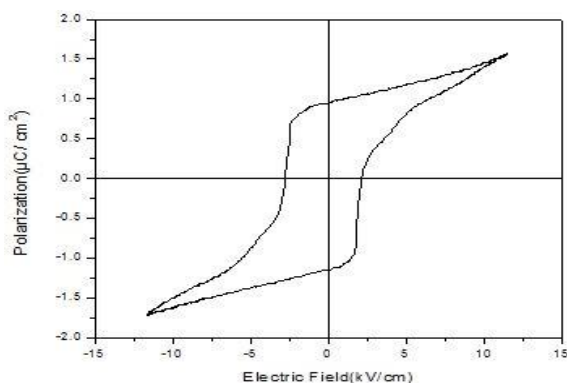


Fig. 6. Ferroelectric P - E hysteresis loop of grown KDP doped TGS crystal.

4. Conclusion

KDP doped TGS crystals of good optical quality were grown by slow evaporation method. UV-Vis spectra show that the grown crystal was optically transparent through 200-800 nm and hence suggests the suitability of this material for optical devices. Powder X-ray diffraction analysis confirms the crystalline nature of grown crystal. The FTIR spectral analysis confirms the presence of functional groups in the crystals. The high optical transparency, and low dielectric constant, proves the suitability of the grown TGS crystal doped with KDP for SHG and other optoelectronic device applications.

Acknowledgements

The authors are thankful to Dr. Binay Kumar, Crystal lab, University of Delhi for Ferroelectric studies and SAIF Kochi for single crystal XRD analysis.

Reference

1. S. Hoshino, Y. Okaya, and R. Pepsinsky, *Phys. Rev.* **115**, 323 (1959).
<http://dx.doi.org/10.1103/PhysRev.115.323>
2. E. M. Mihaylova and H. J. Byrne, *J. Phys. Chem. Solids* **61**, 1919 (2000).
[http://dx.doi.org/10.1016/S0022-3697\(00\)00081-0](http://dx.doi.org/10.1016/S0022-3697(00)00081-0)
3. M. Kay and R. Kliegberg, *Ferroelectrics* **5**, 45 (1973).
<http://dx.doi.org/10.1080/00150197308235778>
4. M. Banan, R. B. Lal and A. K. Batra, *J. Mater. Sci.*, **27**, 2291 (1992).
<http://dx.doi.org/10.1007/BF01105034>
5. K. Meera, R. Muralidharan, P. Santharaghavan, R. Gopalakrishnan, and P. Ramasamy, *J. Cryst. Growth* **226**, 303 (2001). [http://dx.doi.org/10.1016/S0022-0248\(01\)00752-7](http://dx.doi.org/10.1016/S0022-0248(01)00752-7)
6. G. Arunmozhi, S. Lanceros-Mendez, and E. de Matos Gomes, *Mater. Lett.* **54**, 329 (2002).
[http://dx.doi.org/10.1016/S0167-577X\(01\)00588-2](http://dx.doi.org/10.1016/S0167-577X(01)00588-2)
7. A. J. J. Manoharan, N. Joseph John, V. Revathi, K.V. Rajendran, and P. M. Andavan, *Indian J. Sci. Technol.* **4**, 688 (2011).
8. V. N. Shut, I. F. Kashevich, and S. R. Syrtsov, *Phys. Solid State* **50**, 118 (2008).
<http://dx.doi.org/10.1134/S1063783408010216>
9. P. Selvarajan, A. T. H. Sivadas, T. H. Freeda, and C. K. Mahadevan, *Physica B*, **403**, 4205 (2008). <http://dx.doi.org/10.1016/j.physb.2008.09.006>
10. X. Sun, M. Wang, Q. W. Pan, W. Shi, and C. S. Fang, *Cryst. Growth Des.* **34**, 1251 (1999).
11. K. Biedrzycki, *Solid State Commun.* **118**, 141 (2001).
[http://dx.doi.org/10.1016/S0038-1098\(01\)00052-7](http://dx.doi.org/10.1016/S0038-1098(01)00052-7)
12. G. Su, Y. He, H. Yao, Z. Shi, and Q. Wu, *J. Cryst. Growth* **209**, 220 (2000).
[http://dx.doi.org/10.1016/S0022-0248\(99\)00591-6](http://dx.doi.org/10.1016/S0022-0248(99)00591-6)
13. S. Aravazhi, R. Jayavel, and C. Subramanian, *Ferroelectrics* **200**, 279 (1997).
<http://dx.doi.org/10.1080/00150199708008612>
14. R. Renugadevi, G. Kanchana, and R. Kesavasami, *Elixir Crystal Growth* **55A**, 13033 (2013).
15. R W Whatmore, *Rep. Prog. Phys.* **49**, 1335 (1986).
<http://dx.doi.org/10.1088/0034-4885/49/12/002>
16. A. Rahman and J. Podder, *Int. J. Optics*, **86**, 15 (2010).
17. V. Krishnakumar and R. Nagalakshmi, *Spectrochim. Acta, Part A*, **61**, 499 (2005).
<http://dx.doi.org/10.1016/j.saa.2004.04.014> PMID:15582819

18. V. Venkataramanan, S. Maheswaran, J. N. Sherwood, and H. L. Bhat, *J. Cryst. Growth*, **179**, 605 (1997). [http://dx.doi.org/10.1016/S0022-0248\(97\)00137-1](http://dx.doi.org/10.1016/S0022-0248(97)00137-1)
19. V. N. Joshi, *Photoconductivity* (Marcel Dekker, New York, 1990).
20. R. H. Bube, *Photoconductivity of solids* (Wiley, New York, 1981).
21. X. Zhao, C. Sun, Y. Si, M. Liu, D. Xue, *Mod. Phys. Lett.*, **23B**, 3809,(2009).
<http://dx.doi.org/10.1142/S0217984909021867>
22. D. Xue and K. Kitamura, *Ferroelectrics* **297**, 19, (2003).
23. X. Zhang and D. Xue, *J. Phys. Chem. B* **111**, 2587, (2007).
<http://dx.doi.org/10.1021/jp067902s>
24. O. V. Rogazinskaya, S. D. Milovidova, A. S. Sidorkin, A. B. Plaksizkii, A. A. Sidorkin, and T. V. Vorobzhanskaya, *Ferroelectrics* **307**, 255 (2004).
<http://dx.doi.org/10.1080/00150190490493339>